# Extended Lattice Model to Simulate the Printing Process of 3D Printed Cementitious Materials

Chang, Ze; Schlangen, Erik; Šavija, Branko

**DOI**
10.1007/978-3-030-49916-7_80

**Publication date**
2020

**Document Version**
Final published version

**Published in**
Second RILEM International Conference on Concrete and Digital Fabrication

# Extended Lattice Model to Simulate the Printing Process of 3D Printed Cementitious Materials

Ze Chang(✉), Erik Schlangen, and Branko Šavija

Delft University of Technology, Delft, The Netherlands
z.chang-1@tudelft.nl

**Abstract.** This paper reports an extended lattice model for printing process simulation of 3D printed cementitious materials. In this model, several influencing factors such as material and geometric nonlinearity are considered. Using this model, green strength of cementitious material is investigated, deformation and crack pattern can be derived, which is close to the experimental result. Subsequently, numerical analysis of 3D printing is conducted for the simulation about printing process. Imperfections arising in the printing process can be incorporated and two failure modes including the elastic buckling and plastic collapse can be simulated through this model.

**Keywords:** Lattice model · 3D printing · Material nonlinearity · Elastic buckling

## 1 Introduction

Over the past decades, 3D concrete printing (3DCP) gains much attention in the construction industry due to the cost reduction and production rate [1–3].This technology gives capacity to construct the structures by layer-wise extrusion process without using formwork [4]. To search for the suitable printable materials and optimize the printing process, more than 30 research groups worldwide are currently engaged in the research about 3DCP.

In 2008, Thorpe and his co-workers [5, 6] from Loughborough University completed one of the first 3DCP programs named Freeform construction by constructing a gantry-based 3D cementitious materials printer and developing a high performance printable cementitious material. Printable materials should be sufficiently strong, stiff and stable to retain the shape and avoid large deformation under the weight of subsequent layers [7–9]. More recently, explorations have started into many aspects including the printable material compositions and printing scheme. A fundamental understanding of printable materials and printing process has developed via two parameters: “open time” for printable materials (open time is the period where the mechanical properties meet the printing requirement) and the “buildability” for the printing process (Buildability is that the object can be successfully built without failure and large deformation) [7, 10–15].


F. P. Bos et al. (Eds.): DC 2020, RILEM Bookseries 28, pp. 814–823, 2020.
https://doi.org/10.1007/978-3-030-49916-7_80

Albeit a steadily growing number of researchers active in the 3DCP research, numerical and theoretical models are still in their infancy. Roussel [19, 22, 23] investigated the rheological and thixotropic characteristics of cementitious materials and established the linear strength evolution with hydration time. An analytical model based on material rheology [19] was ultimately proposed to evaluate the printability of cementitious materials [16–20]. This analytical model, which has been experimentally validated, can predict the maximum number of printing layers considering the plastic collapse failure mode. Successive developments of this model can be found in the literature [5, 15–19, 22, 24]. The plastic collapse failure mode can be well predicted using such analytical models. But some issues still remain. The other failure mode (i.e. elastic buckling) is ignored in analytical models since the influence of structural geometry is not considered. Confronted with this research gap, a mechanistic model was proposed by Suiker [21] for the analysis of elastic buckling and plastic collapse. This mechanistic model was derived using a combination of energy theory, equilibrium equations and boundary conditions. The geometric imperfections generated during printing of a wall was included in the buckling model by decomposing the dimensionless deflection. Experiments were used to validate numerical results, which underestimated the total number of filament layers by 10%. Furthermore, the mechanistic model was limited to the straight wall structural geometry. To propose a more versatile model, Wolfs et al. [9, 25] investigated the mechanical properties of cementitious materials at an early stage and hardened stage through a uniaxial compression test and a direct shear test to derive the mechanical properties in numerical simulations. Based on the experimental results, numerical analyses of the green strength and the printing process of cementitious materials were conducted using commercial software ABAQUS [9]. The model yielded reasonable results, with 25% overestimation of the total number of filament layers compared to the experimental results. Importantly, by using this numerical model, the correct failure modes such as elastic buckling and plastic collapse were predicted. From the review of current research, it can be stated that all listed models show great progress in evaluating the buildability and printability of cementitious materials. However, some issues still exist in these models. For instance, most models ignore important influencing factors such as imperfections, plastic shrinkage, and creep, among others. A more reasonable numerical model is necessary for optimizing the printing process and guiding a real 3D printed project.

Lattice model, based on the discontinuous formulation, can avoid singularity-related issues in continuum-based numerical methods. Besides, the imperfection during the printing process can be easily implemented in the lattice model. Herein, the lattice model is utilized as the basic model to do specific improvements to meet the requirements of 3DCP numerical analysis.

In this paper, the extended lattice model is proposed for numerical analysis of the printing process of 3DCP. The proposed model takes the geometric and material nonlinearity into account. The model is used to simulate the green strength and the printing process. This paper can be divided into 3 main parts. In the first section, basic theory of the lattice fracture model is briefly introduced and some improvements on the lattice model for considering nonlinearity and non-proportional loading are explained for 3D printing simulation. In the second part, the green strength of cementitious material is simulated for the calibration of local mechanical properties of 3D printed concrete. Finally, using the obtained input parameters, the simulation of the 3D printing is performed, showing the capability of the model to capture the typical failure modes.

## 2 Model Development

### 2.1 Lattice Model

In the lattice fracture model, the material is discretized by a network of Timoshenko beam elements, which are constituted by the random nodes in a limited domain through the Delaunay triangulation [26]. The schematic view of lattice model generation for 3D printing can be found in Fig. 1. In lattice model, the Timoshenko beam element is generally used to model shear deformation considering the low ratio of length and height of the beam elements in the lattice model.

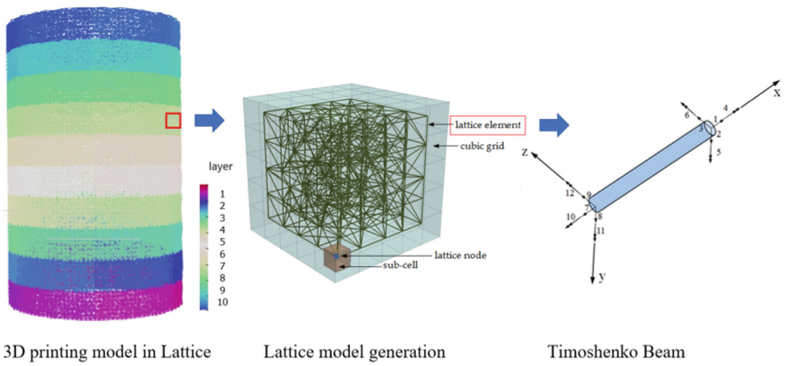


**Fig. 1.** Schematic view of lattice model generation for 3D printing

In lattice fracture model, the element strength and stiffness are obtained by calibration of experimental data [26, 28, 29]. Using these mechanical properties, a set of linear elastic analysis is performed through the calculation of stress distribution for each element subjected to an imposed particular load. The element with the highest stress/strength ratio is regarded as the critical element and removed from the lattice mesh, thereby introducing a small crack [26]. Once the critical element is found, the mechanical properties change and the global stiffness matrix is updated due to the damage. The step-by-step removal presents the initiation and propagation of the crack, finally, crack pattern of the lattice model could be obtained. Meanwhile, the displacement of the model, calculated by scaling factor and prescribed displacement, determines the load-displacement curve of the model.

Based on the Timoshenko beam theory, the element is a lattice beam of uniform cross-section and can transfer the uniaxial force, shear, bending and torsion [27]. The stress for the lattice element is calculated by the following equation.

$$\sigma = \frac{F}{A} + \alpha \frac{(|M_i|, |M_j|)_{\max}}{W} \tag{1}$$

Where $F$ is the normal force for the lattice beam element, $M_i$ and $M_j$ are the local bending moment in local coordinate system, $A$ is the cross-sectional area of an element, and $W = \pi D^3/32$ the section modulus of an element ($D$ is the diameter of the circle area). The coefficient $\alpha$ is the bending influence factor which balances the final failure mode in which either force or bending plays a dominant role. According to previous research [26, 28, 29], the value of the bending influence factor is set to 0.05.

## 2.2 Extended Lattice Model

The lattice fracture model for fracture analysis of cementitious materials has been proposed by Schlangen [26, 28, 29]. This model is generally based on the sequentially-linear analysis procedure, and each element has brittle behaviour.

In lattice fracture model, the element step wise constitutive relationships are calibrated by fitting the global load and displacement curve to represent elastic-plastic behaviour (see Fig. 2). In every analysis step, loading or displacement is increased until one beam in the model has the stress/strength ratio equal to one. This critical element weakens and reduced stiffness is set to the element for the next step calculation. When reaching the last step in the constitutive relationship, this beam is removed from the system. The loading procedure is increasing until a predefined stop criterion (e.g. load or displacement).

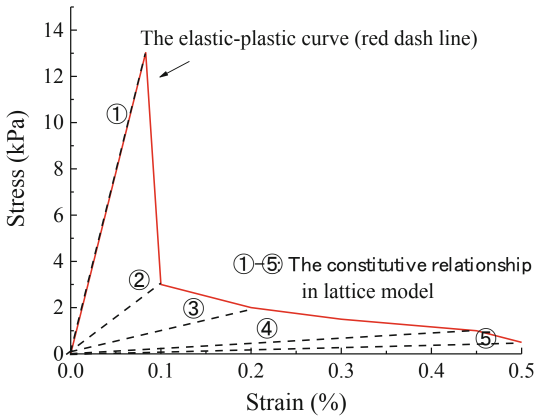


**Fig. 2.** The elastic-plastic constitutive relationship in lattice model

The second improvement is related to non-proportional loading. After extrusion, the self-weight of previous layers remains in the system, resulting in an internal force among in the lattice elements. When the following layer is printed, the prescribed load increment results in failure of additional elements, which causes stress redistribution. To overcome this issue, the improved sequentially linear solution, proposed by the Eliáš [30], is incorporated into the lattice model.

Another improvement is the consideration of the geometric nonlinearity. Apart from the removed or degraded elements, the nodal displacements' variation in the lattice system also results in the disequilibrium force. After occurrence of the force, a sequentially linear redistribution process of stress release takes place until a static equilibrium state reaches.

Taking these influencing factors into consideration, the extended lattice model is used for simulation of 3D printing.

## 3 Numerical Analysis

The numerical analysis of 3DCP is investigated in two steps using the extended lattice model. The first step concerns calibration of the local mechanical properties by simulating the compression test. A case in point, the element mechanical properties for the simulation of green strength in 30-min is as shown in Fig. 2. In the second step the extended lattice model is utilized to simulate the structural behaviour during the printing process and research the failure-deformation mode.

### 3.1 Compression Test

The extended lattice model is used to analyse the green strength (the compressive strength obtained from such mortar cylinders in fresh state is commonly called green strength of the tested material) and deformation characteristics of fresh cementitious material, relying on the experimental results from Chen et al. [12, 13].

In their experiment, cylinder specimens with diameter of 33.5 mm and height of 67.5 mm are utilized for the investigation of green strength. In the numerical analysis, the displacement in vertical direction is applied to the top of edge of the cylinder, which corresponds to 15% vertical strain. The bottom is simply supported in vertical direction. The step-wise constitutive relationship is utilized to represent the elastic-plastic mechanical constitutive relation in extended lattice model.

The numerical analysis for cementitious materials is performed for each stage in the experimental program. The calibrated mechanical properties are as shown in Table 1. The resulting load-displacement diagram in loading direction is compared with the experimental results, see Fig. 3. The simulation results (in solid line) agree well with the experimental finding (in dash line). Besides, the global deformation of the specimen ($t$ = 40 min) and the crack patterns for the sample ($t$ = 4 h) keep the same with the experimental diagram. Therefore, the extended lattice model is deemed possible to model the green strength and deformation characteristic of fresh cementitious materials.

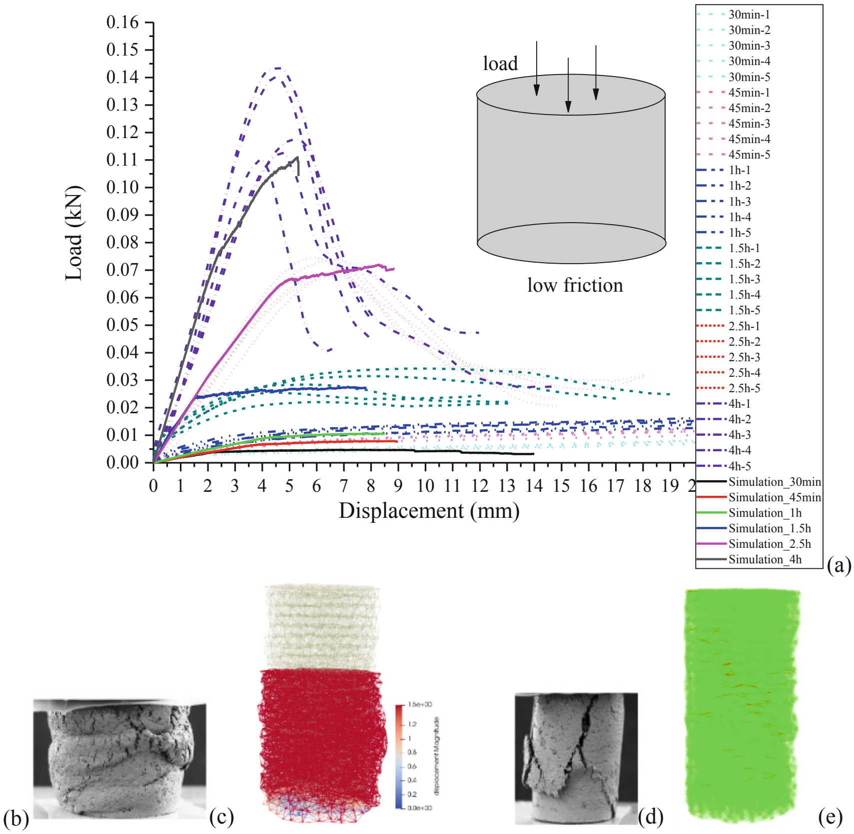


**Fig. 3.** The comparison between the numerical result and experimental results (a) load-displacement curve (b) Deformation from literature [13] (c) Deformation in numerical analysis (d) Crack pattern from literature [13] (e) Crack pattern in numerical analysis

**Table 1.** Calibrated element mechanical properties in lattice model

| Time/min | Segments | Part 1 (kPa) | | Part 2 (kPa) | | Part 3 (kPa) | | Part 4 (kPa) | | Part 5 (kPa) | | Part 6 (kPa) | |
|---|---|---|---|---|---|---|---|---|---|---|---|---|---|
| | | $E$ | $F_c$ | $E$ | $F_c$ | $E$ | $F_c$ | $E$ | $F_c$ | $E$ | $F_c$ | $E$ | $F_c$ |
| 30 | 6 | 161 | 8 | 33 | 8 | 19 | 8 | 13 | 8 | 10 | 8 | 8 | 8 |
| 45 | 6 | 157 | 13 | 49 | 13 | 29 | 13 | 21 | 13 | 16 | 13 | 13 | 13 |
| 60 | 5 | 197 | 18 | 67 | 18 | 40 | 18 | 29 | 18 | 23 | 18 | | |
| 90 | 6 | 1461 | 50 | 222 | 50 | 120 | 50 | 82 | 50 | 63 | 50 | 13 | 13 |
| 150 | 4 | 1261 | 128 | 478 | 128 | 295 | 128 | 213 | 128 | | | | |
| 240 | 2 | 2705 | 240 | 1200 | 240 | | | | | | | | |

## 3.2 Printing Process

The overview of printing process parameters for cylinder and wall structure are listed in Table 2. In both numerical analyses, the bottom layers are taken as fixed, assuming high friction in printing bed. Each node in the extended lattice model has gravity representing the self-weight of the printable materials. The element mechanical properties of each layer are assumed to be constant, which should be calculated during the analysis based on their age in the printing process, for instance, after 5 layers, the initial layer will be 32.5 min old and use the corresponding mechanical properties of that age, while the last printing layer should be 30 min old, and so on. Since in this paper, the model time for the designed project is less than 5 min, the strength and stiffness are assigned as constant.

**Table 2.** The input parameters for the models

| | Parameter | Value |
|---|---|---|
| Wall structure | Wall thickness (w) | 12 mm |
| | Wall length (l) | 200 mm |
| | Height for each layer (h) | 7 mm |
| | Printing speed | 30 s/layer |
| Cylinder structure | Heart radius | 62 mm |
| | Thickness for each layer | 13 mm |
| | Height of each layer | 6 mm |
| | Printing speed | 30 s/layer |

For the wall structure, two imperfections are introduced to the wall structure model to investigate the imperfection influence on the final failure mode, in which 8th and 10th layers are subjected 1.5 mm horizontal shift.

Two numerical models are investigated to study structures with different geometry and the impact of imperfections during the printing process. Figure 4 shows the initial structure and the deformed model towards different printing shape. For the cylinder structure, due to the restrained deformation in the radial direction, a tendency of cylinder buckling occurs, which is a combination of elastic buckling and plastic collapse. The subsequent printing layers increase the element stress and strain due to the increasing self-weight in the model. At this point, some elements meet the failure criteria and are removed from the model. Therefore, the system becomes unstable and the tendency for elastic buckling are more obvious. For the wall structure, a more obvious elastic buckling can be observed due to the horizontal shift in the $6^{th}$ and the $10^{th}$ layer. After the $12^{th}$ layer, the imperfections cause the system to lose its capacity to bear the load from subsequent printing layers and the model eventually fails.

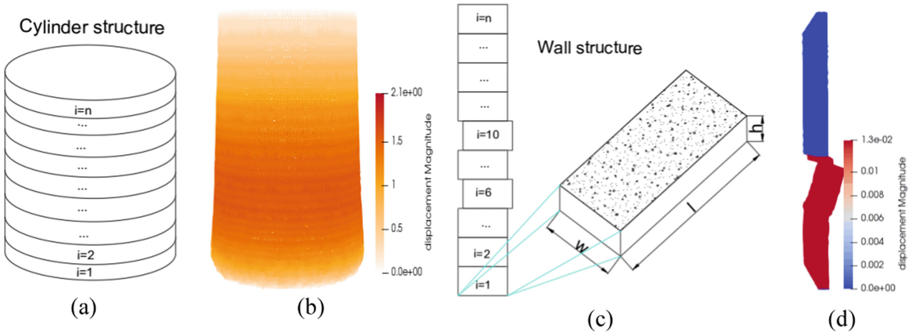


**Fig. 4.** (a) Hollow cylinder (b) Failure mode about the hollow cylinder (c) Wall structure (d) Failure mode about the wall structure

## 4 Conclusions

In this paper, an extended lattice model is proposed to simulate the green strength of cementitious materials, in the range of 30-min to 4-h after adding water. Subsequently, the printing process is simulated using the input parameters derived by the calibration of the compression test. Based on the presented results, the following conclusions can be formulated.

- The extended lattice model is able to model the green strength and deformation characteristics of fresh cementitious materials;
- The structural behaviour of cementitious material during 3D printing can be simulated and the corresponding failure-deformation mode can be derived using this model.
- Finally, it may be concluded that the extended lattice model is suitable to simulate 3D printing of concrete. As further work, the model should be validated by comparison to printing experiments. Besides, more influence factors such as plastic shrinkage will be introduced into the model and the model will be further utilized as a numerical tool for the optimization of 3D printing.

**Acknowledgements.** Ze Chang would like to acknowledge the funding supported by China Scholarship Council under grant number 201806060129.

## References

1. Bos, F., Wolfs, R., Ahmed, Z., Salet, T.: Additive manufacturing of concrete in construction: potentials and challenges of 3D concrete printing. Virtual Phys. Prototyping **11**(3), 209–225 (2016)
2. Buswell, R.A., de Silva, W.L., Jones, S., Dirrenberger, J.: 3D printing using concrete extrusion: a roadmap for research. Cem. Concr. Res. **112**, 37–49 (2018)

3. Gebler, M., Schoot Uiterkamp, A.J.M., Visser, C.: A global sustainability perspective on 3D printing technologies. Energy Pol. **74**, 158–167 (2014)
4. Tay, Y.W.D., Panda, B., Paul, S.C., Noor Mohamed, N.A., Tan, M.J., Leong, K.F.: 3D printing trends in building and construction industry: a review. Virtual Phys. Prototyping **12** (3), 261–276 (2017)
5. Lim, S., Buswell, R.A., Le, T.T., Austin, S.A., Gibb, A.G., Thorpe, T.: Developments in construction-scale additive manufacturing processes. Autom. Constr. **21**, 262–268 (2012)
6. Le, T.T., Austin, S.A., Lim, S., Buswell, R.A., Gibb, A.G., Thorpe, T.: Mix design and fresh properties for high-performance printing concrete. Mater. Struct. **45**(8), 1221–1232 (2012)
7. Panda, B., Unluer, C., Tan, M.J.: Investigation of the rheology and strength of geopolymer mixtures for extrusion-based 3D printing. Cem. Concr. Compos. **94**, 307–314 (2018)
8. Perrot, A., Rangeard, D., Pierre, A.: Structural built-up of cement-based materials used for 3D-printing extrusion techniques. Mater. Struct. **49**(4), 1213–1220 (2015)
9. Wolfs, R., Bos, F., Salet, T.: Early age mechanical behaviour of 3D printed concrete: numerical modelling and experimental testing. Cem. Concr. Res. **106**, 103–116 (2018)
10. Kazemian, A., Yuan, X., Cochran, E., Khoshnevis, B.: Cementitious materials for construction-scale 3D printing: laboratory testing of fresh printing mixture. Constr. Build. Mater. **145**, 639–647 (2017)
11. Paul, S.C., Tay, Y.W.D., Panda, B., Tan, M.J.: Fresh and hardened properties of 3D printable cementitious materials for building and construction. Arch. Civil Mech. Eng. **18**(1), 311–319 (2018)
12. Chen, Y., Chaves Figueiredo, S., Yalçinkaya, Ç., Çopuroğlu, O., Veer, F., Schlangen, E.: The effect of viscosity-modifying admixture on the extrudability of limestone and calcined clay-based cementitious material for extrusion-based 3d concrete printing. Materials **12**(9), 1374 (2019)
13. Chen, Y., Li, Z., Chaves Figueiredo, S., Çopuroğlu, O., Veer, F., Schlangen, E.: Limestone and calcined clay-based sustainable cementitious materials for 3D concrete printing: a fundamental study of extrudability and early-age strength development. Appl. Sci. **9**(9), 1809 (2019)
14. Ma, G., Li, Z., Wang, L.: Printable properties of cementitious material containing copper tailings for extrusion based 3D printing. Constr. Build. Mater. **162**, 613–627 (2018)
15. Weng, Y., Li, M., Tan, M.J., Qian, S.: Design 3D printing cementitious materials via Fuller Thompson theory and Marson-Percy model. Constr. Build. Mater. **163**, 600–610 (2018)
16. Kruger, J., Cho, S., Zeranka, S., Viljoen, C., van Zijl, G.: 3D concrete printer parameter optimisation for high rate digital construction avoiding plastic collapse. Compos. Part B Eng. **183**, 107660 (2020)
17. Kruger, J., Zeranka, S., van Zijl, G.: 3D concrete printing: a lower bound analytical model for buildability performance quantification. Autom. Constr. **106**, 102904 (2019)
18. Perrot, A., Rangeard, D., Pierre, A.: Structural built-up of cement-based materials used for 3D-printing extrusion techniques. Mater. Struct. **49**(4), 1213–1220 (2016)
19. Roussel, N.: A thixotropy model for fresh fluid concretes: theory, validation and applications. Cem. Concr. Res. **36**(10), 1797–1806 (2006)
20. Roussel, N., Ovarlez, G., Garrault, S., Brumaud, C.: The origins of thixotropy of fresh cement pastes. Cem. Concr. Res. **42**(1), 148–157 (2012)
21. Suiker, A.S.J.: Mechanical performance of wall structures in 3D printing processes: theory, design tools and experiments. Int. J. Mech. Sci. **137**, 145–170 (2018)
22. Kovler, K., Roussel, N.: Properties of fresh and hardened concrete. Cem. Concr. Res. **41**(7), 775–792 (2011)
23. Roussel, N.: Rheology of fresh concrete: from measurements to predictions of casting processes. Mater. Struct. **40**(10), 1001–1012 (2007)

24. Wangler, T., Lloret, E., Reiter, L., Hack, N., Gramazio, F., Kohler, M., Bernhard, M., Dillenburger, B., Buchli, J., Roussel, N.: Digital concrete: opportunities and challenges. RILEM Techn. Letters **1**, 67–75 (2016)
25. Wolfs, R., Bos, F., Salet, T.: Hardened properties of 3D printed concrete: the influence of process parameters on interlayer adhesion. Cem. Concr. Res. **119**, 132–140 (2019)
26. Qian, Z., Schlangen, E., Ye, G., van Breugel, K.: Modeling framework for fracture in multiscale cement-based material structures. Materials **10**(6), 587 (2017). Basel
27. Liu, D., Šavija, B., Smith, G.E., Flewitt, P.E.J., Lowe, T., Schlangen, E.: Towards understanding the influence of porosity on mechanical and fracture behaviour of quasi-brittle materials: experiments and modelling. Int. J. Fract. **205**(1), 57–72 (2017)
28. Schlangen, E., Garboczi, E.J.: Fracture simulations of concrete using lattice models: computational aspects. Eng. Fract. Mech. **57**(2–3), 319–332 (1997)
29. Chang, Z., Zhang, H., Schlangen, E., Šavija, B.: Lattice Fracture Model for Concrete Fracture Revisited: Calibration and Validation. Submitted for publication (2019)
30. Eliáš, J., Frantík, P., Vořechovský, M.: Improved sequentially linear solution procedure. Eng. Fract. Mech. **77**(12), 2263–2276 (2010)